



# A highly sensitive ammonia sensor based on spinous core–shell PCL–PANI fibers

Wei Zhou<sup>1</sup>, Yutong Guo<sup>1</sup>, Hui Zhang<sup>1,\*</sup>, Yajun Su<sup>1</sup>, Mei Liu<sup>1</sup>, and Bin Dong<sup>1,\*</sup>

<sup>1</sup>Institute of Functional Nano & Soft Materials (FUNSOM), Jiangsu Key Laboratory for Carbon-Based Functional Materials & Devices, Soochow University, Suzhou 215123, Jiangsu, People's Republic of China

**Received:** 9 September 2016

**Accepted:** 3 February 2017

**Published online:**

1 March 2017

© Springer Science+Business Media New York 2017

## ABSTRACT

In this paper, we report a unique hierarchical core–shell polycaprolactone–polyaniline fiber with spinous surface structures, which is fabricated by direct in situ oxidative polymerization of aniline on the surface of porous electrospun PCL fibers. Due to the high surface area-to-volume ratio caused by the hierarchical structure, when utilized for ammonia gas sensing, the resulting core–shell fibers exhibit high sensitivity, which is far superior to that of the film or the smooth fiber counterparts. In addition, the sensor based on the current structure is extremely sensitive to the ammonia gas, which is evidenced by the fast response time (20 s) and the low detection limit (1 ppm). Moreover, the sensor not only shows good repeatability when repetitively exposing it to the ammonia gas but also exhibits good selectivity toward ammonia over other common volatile organic compounds. We thus believe the structure reported in the current study may have potential applications in the field of ammonia gas sensor.

## Introduction

Conducting polymers have attracted more and more attentions in recent years. Due to their conjugated backbones, they are electrically conductive in nature. Because of their unique structures and properties, they can be utilized as active materials for light-emitting diode or polymer solar cell [1]. In addition, they can also be utilized as the electrode material for lithium-ion battery based on their charging and

recharging properties [2]. Since the doping level of the conducting polymer is tunable, which is subject to the surrounding environment, the conducting polymer is considered as an attractive candidate for sensors [3]. Among others, ammonia sensing based on the conducting polymers has been extensively explored because of the high toxicity of ammonia and the good sensitivity of the conducting polymers toward the ammonia gas [4, 5]. When utilized as an active sensing material, polyaniline (PANI) exhibits much higher sensitivity when compared with

Wei Zhou and Yutong Guo have contributed equally to this work.

Address correspondence to E-mail: huizhang@suda.edu.cn; bdong@suda.edu.cn

polypyrrole. The high sensitivity of PANI-based ammonia sensor originates from the ammonia-induced deprotonation process, which causes the decrease in the carrier density and the sharp change in resistance [6].

In order to improve the sensitivity of PANI, it is often fabricated into microstructures, which may increase its surface area-to-volume ratio and facilitate the sensing performance of the sensor device. Among others, bottom-up oxidative polymerization method has already been utilized to obtain PANI microstructures [7]. For example, Kaner et al. have developed a PANI nanowire-based ammonia sensor through the interfacial polymerization method [8]. Chen et al. have constructed a flexible and transparent ammonia gas sensor by in situ oxidative polymerization of aniline on the surface of functional multiwalled carbon nanotubes [9]. However, it is difficult to manipulate and locate the PANI nanowires synthesized by the oxidative polymerization with respect to the microelectrodes. An alternative way to obtain the PANI microstructure is based on electrospinning [10]. Electrospinning is a method widely utilized to obtain polymer fibers out of their solutions or melts [11–14]. By utilizing electrospinning method, Craighead et al. have successfully fabricated a PANI fiber-based ammonia gas sensor with the aid of polyethylene oxide carrier polymer [15]. Despite this progress, the resulting electrospun fiber has limited surface area. Therefore, in order to overcome the problems mentioned above, it is desirable to combine the advantages of the two methods above and develop fiber-based hierarchical structures.

In this paper, we have fabricated a hierarchical PANI fibrous structure by combining the oxidative polymerization with the electrospinning method. PANI is directly deposited on the surface of electrospun porous polycaprolactone (PCL) fibers. By controlling the polymerization time, a unique spinous core-shell fiber can be obtained. The resulting hierarchical structures can greatly improve the surface area-to-volume ratio of PANI. As a result, when utilized in ammonia gas sensor, it shows high sensing performance, which is much higher when compared to that of the smooth fiber or the film counterpart. In addition to the high sensitivity, the sensing device also exhibits fast responsibility, low detection limit, good repeatability and selectivity. We thus believe the hierarchical structure reported in the current

study is potentially attractive for ammonia-gas-sensing applications.

## Experimental

### Materials

Ammonium persulfate (APS) and PCL were obtained from Sigma-Aldrich Company. Aniline, *N,N*-dimethylformamide (DMF) and concentrated hydrochloric acid were obtained from J&K Scientific. Methanol, ethanol, isopropanol, dichloromethane, chloroform, acetone and acetic acid were obtained from Sinopharm Chemical Reagent Co., Ltd. All reagents were used without further purification.

### Preparation of PCL fiber

PCL fiber is obtained by electrospinning method. First, PCL was dissolved in chloroform at a mass fraction of 10 wt%. The solution was loaded into a syringe with a 21-gauge blunt needle, which was then placed on a syringe pump (Longer Pump Lspol-1A). The needle end was connected to a high-voltage power supply. During the electrospinning process, the polymer solution was pumped at the rate of 60  $\mu\text{L min}^{-1}$ . The separation distance between the needle and the collector was fixed at 10 cm. Once a high voltage (11 kV) was applied, a Taylor cone was formed at the needle end and the polymer solution was ejected toward the grounded collector. Once the solvent evaporated, the porous fiber structure was formed on the collector. The smooth fiber was obtained in a similar fashion except the 1:1 DMF/chloroform (V/V) was utilized as the solvent instead of the pure chloroform.

### Preparation of hierarchical PCL–PANI core-shell structure

We utilized the in situ oxidative polymerization method to obtain a hierarchical PCL–PANI structure. In a typical experiment, 1 mmol aniline monomer was first added into 10 mL 1 M HCl aqueous solution, which was cooled at 5 °C after the ultrasonication treatment. The electrospun porous PCL fiber was immersed into the aniline solution for 15 min. Ten milliliter pre-cooled 1 M HCl aqueous solution with 1 mmol ammonium persulfate was added into the

above solution. The mixture was left at 5 °C for different periods of time. The fiber was then taken out and thoroughly washed with ethanol and dried at room temperature. The PANI film and PANI deposited on the smooth fiber were fabricated by the same method as two control samples.

## Characterizations

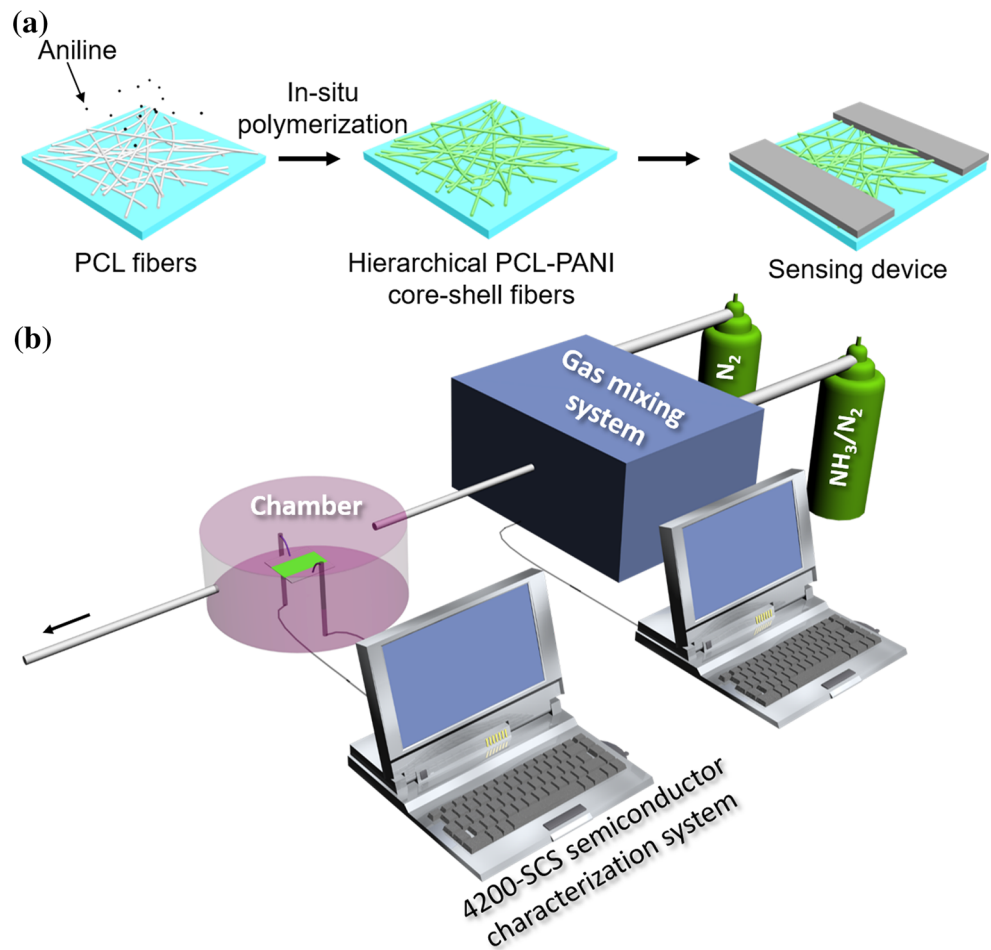
The morphologies of the hierarchical structures were studied by using a scanning electron microscopy (SEM) (Carl Zeiss Supra 55). Prior to the SEM observation, a thin layer of gold was sputtered. Raman measurement was taken on a Horiba Jobin-Yvon LabRAM HR800 Raman spectrometer. A 514-nm laser was applied for excitation. Fourier transform infrared (FTIR) spectra were collected on a Hyperion FTIR spectrometer (Bruker). For the gas-sensing experiment, the PCL–PANI fiber was connected to the probes of Keithley 4200-SCS semiconductor

characterization system with silver paint. The sensing device was then placed in a small chamber. Different concentrations of ammonia or other volatile organic gases, which was obtained through RCS 2000-A gas-mixing system (Forest Voice Technology), were applied into this chamber, and the changes in the resistance were recorded. All measurements were taken at room temperature.

## Results and Discussion

The fabrication process is illustrated in Fig. 1a. A porous fiber consisting of PCL is first obtained by electrospinning method. In situ oxidative polymerization of aniline is performed on the fiber surface, resulting in the formation of hierarchical structures. During this process, the original white-colored PCL fiber turns into green, which indicates the deposition of PANI. The resulting hierarchical fibers are then

**Figure 1** **a** Schematic illustrating the preparation of the gas-sensing device. **b** Schematic illustrating the gas-mixing system, the measurement chamber and the gas-sensing characterization system.



placed between two electrodes to examine the electrical property and evaluate the sensing performance. We have utilized a system shown in Fig. 1b to obtain the sensing behavior of the fiber-based sensor. RCS 2000-A gas-mixing system, which is a computerized device that automatically provides mixed gas from gas sources with a concentration down to ppb level, is used to obtain the ammonia gas with certain concentrations.

In order to construct a hierarchical structure, a porous fiber is first obtained by electrospinning method. Electrospinning is known to be a method to process polymer solutions into different microstructures. By adjusting the electrospinning parameters (polymer solution concentration, solvent, voltage, pump speed, separation distance between the tip and the collector, etc.), a variety of polymer structures can be obtained, including bead, beaded fiber, fiber [16–18]. In the current study, we select PCL as the polymeric material and utilize a low boiling point solvent (chloroform). The electrospinning of the PCL's chloroform solution results in the formation of porous polymeric fibers, as illustrated in Fig. 2a. The solution concentration, voltage, separation distance and pumping rate are 10 wt%, 11 kV, 10 cm and  $60 \mu\text{L min}^{-1}$ , respectively. The formation of the

porous structure is likely due to the rapid phase separation caused by the solvent evaporation and the subsequent solidification of the polymer [19]. Figure 2b and c shows the typical SEM images of the porous fibers. The pores on the fiber have an average size of approximately  $1 \mu\text{m}$ .

We then perform the in situ oxidative polymerization of aniline on the PCL porous fibers. As indicated in Fig. 3, PANI can be deposited onto the fiber surface, which is likely due to the hydrophobic nature of both PANI and PCL. Figure 3a–d shows a series of SEM images indicating the structures obtained at different deposition time. PANI forms a smooth coating on PCL surface at 1-h polymerization time (Fig. 3a). When the deposition time is 2 h, in addition to the PANI film, several outgrown nanoparticles distribute sparsely on the fiber surface (Fig. 3b). When the time increases to 4 h, hierarchical PCL–PANI fiber is formed, as indicated in Fig. 3c. It is worth pointing out that the structure obtained at 4-h polymerization time not only preserves the porous structures (i.e., the pores are still observable) but also exhibits a new feature (i.e., PANI starts to grow out of the fiber to form spinous structures), resulting in the formation of the hierarchical fibers. When further increasing the deposition time to 6 h, thicker

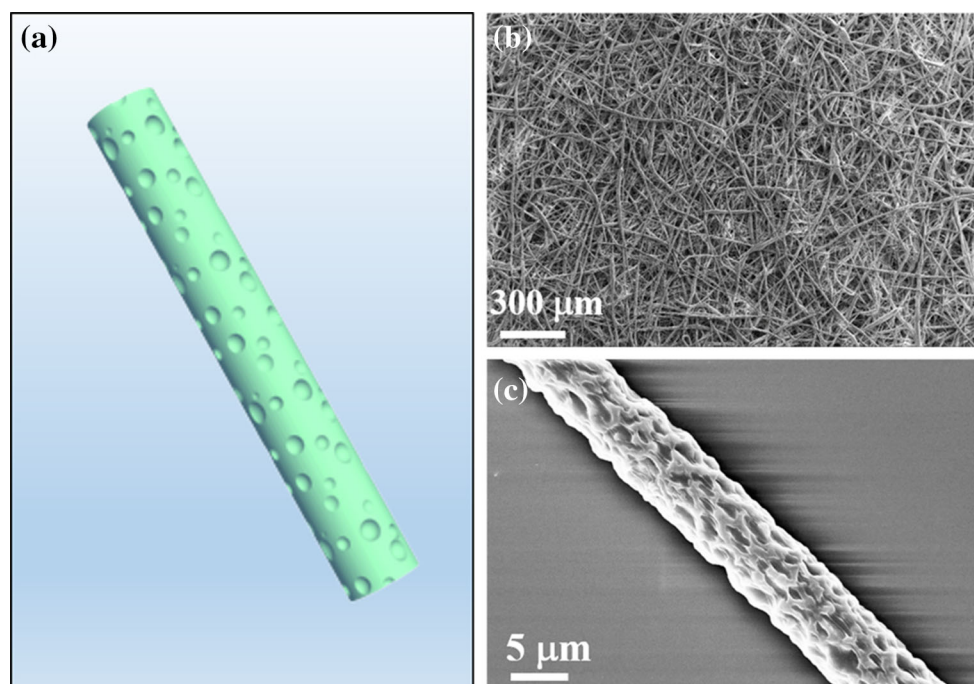


**Figure 2** a Schematic image of the porous PCL fiber. b The SEM image of the PCL fibrous mat. c An enlarged SEM image shows a single fiber.

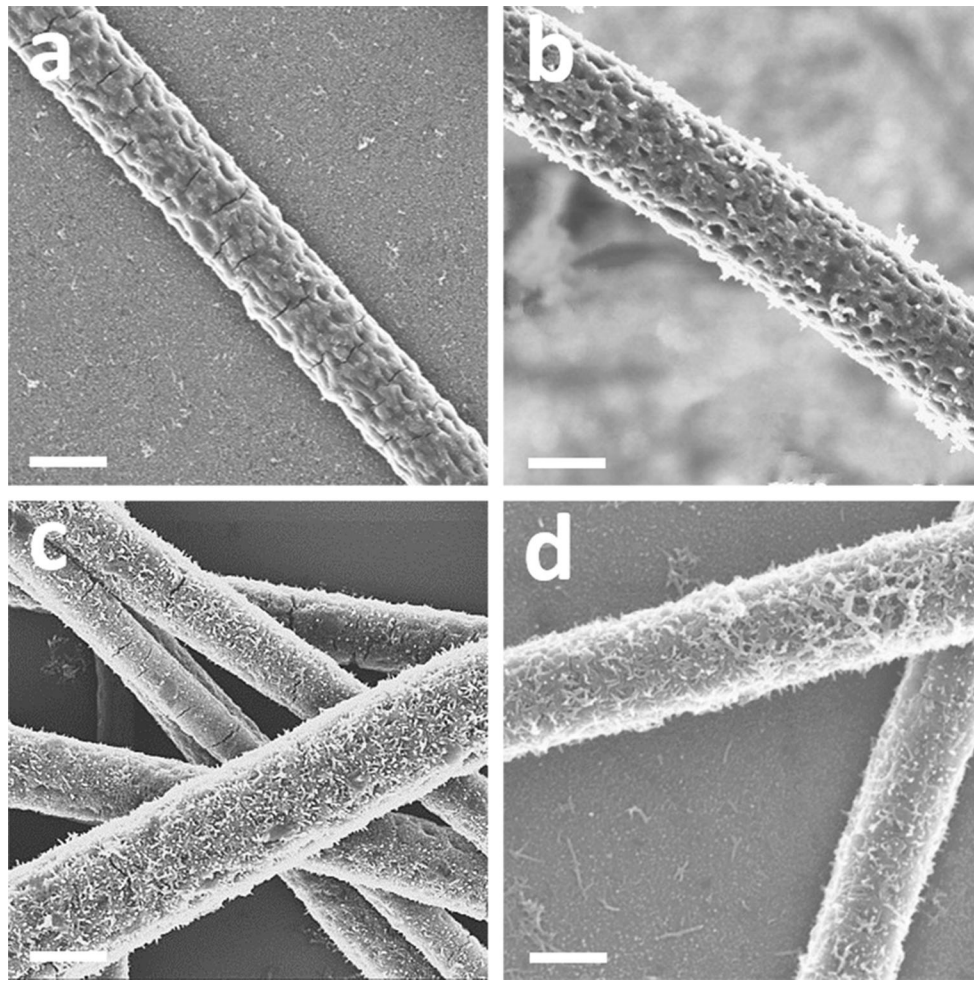


**Figure 3** SEM images of hierarchical PCL–PANI fibers obtained at the polymerization time of **a** 1 h, **b** 2 h, **c** 4 h and **d** 6 h, respectively. The scale bar is 3  $\mu\text{m}$ .

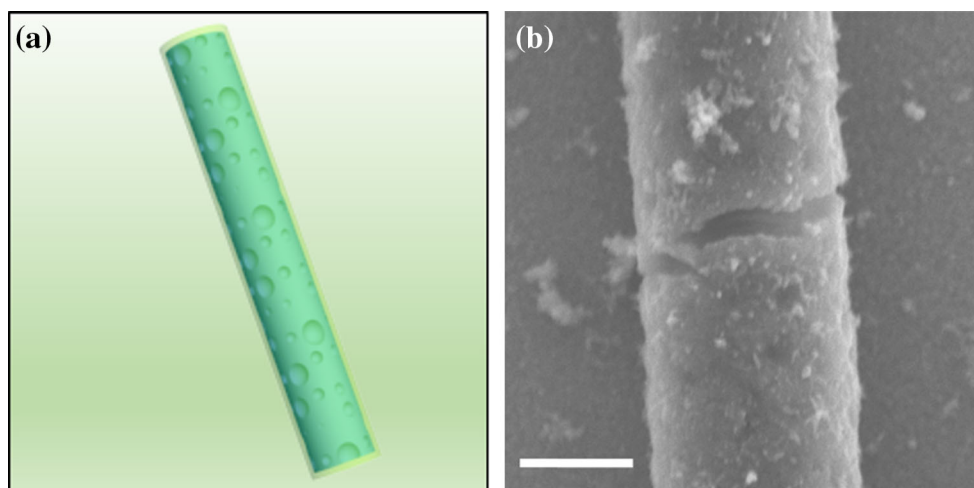


**Figure 4** **a** Schematic illustrates the core–shell structure of PCL–PANI fiber. **b** The SEM image of the fractured fiber indicating the core–shell structure. The scale bar is 2  $\mu\text{m}$ .

coating is formed on the fiber surface, as shown in Fig. 3d. Due to the long polymerization time, the pores on the fibers are barely visible.

We believe the PCL–PANI fiber possesses a core–shell structure (Fig. 4a). In order to confirm this, we have fractured the fiber and examined it under the SEM. Figure 4b shows a typical SEM image of one broken fiber. It can be seen that the inner fiber is surrounded by a thin outer shell, thus demonstrating the core–shell structure.

The TEM images shown in Fig. 5 further confirm the core–shell structure of the PCL–PANI fiber, i.e., the inner PCL fiber, is surrounded by a thin layer of PANI. In addition, as the polymerization time increases, the shell layer becomes thicker. The shell thickness increases from approximately 12 nm in the case of 1-h polymerization time to around 80 nm in the case of 6-h polymerization time.

In addition, for the comparison purpose, we have performed two control experiments. One is to deposit PANI films on the substrate surface in the absence of the PCL fibers. For this control experiment, by adjusting the polymerization time, we have obtained PANI films with different morphologies and examined them by utilizing SEM. Figure 6a–d shows the PANI films obtained at 1-h, 2-h, 4-h and 6-h deposition time, respectively. It can be seen from these figures that the film consists of many PANI nanoparticles. As the deposition time increases, the PANI nanoparticles gradually accumulate, forming denser films.

The other control experiment is to deposit PANI on the smooth PCL fiber. We find out the formation of the porous fiber is highly dependent on the solvent. When we utilize 1:1 DMF/chloroform (V/V) as the solvent instead of the pure chloroform, only smooth

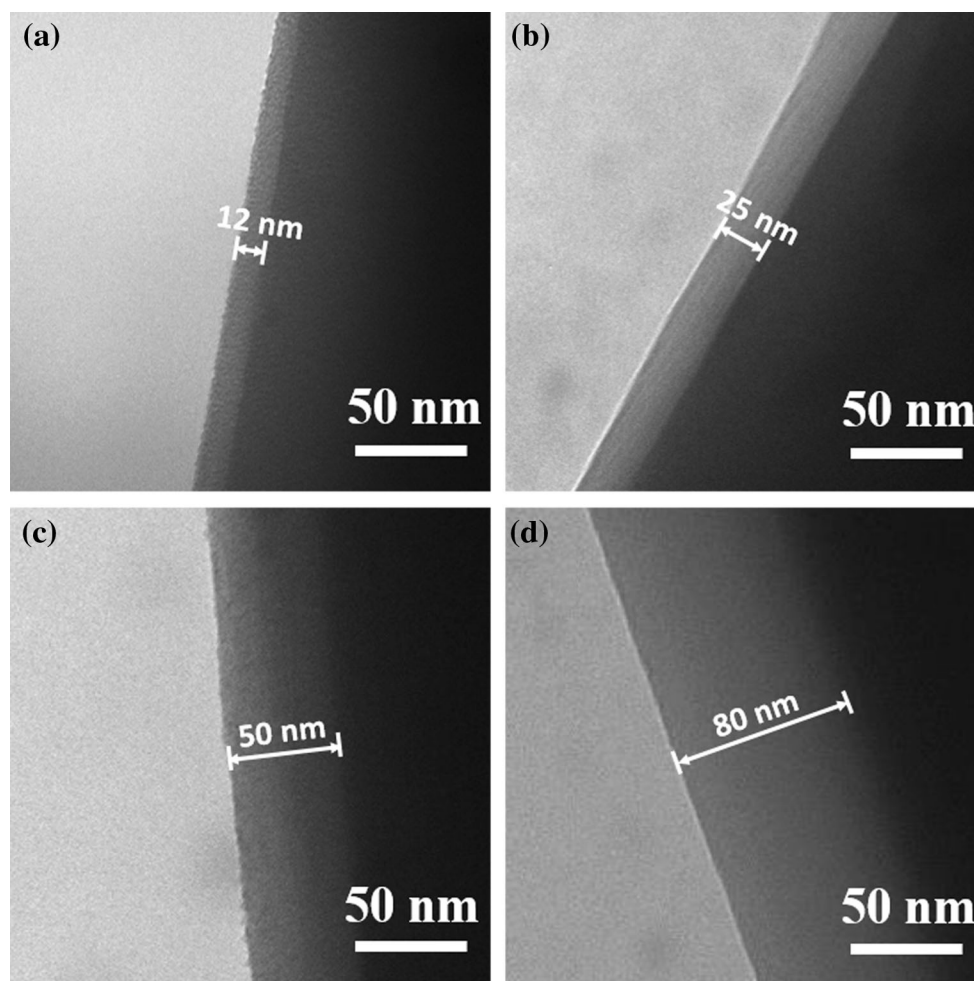


**Figure 5** TEM images of the hierarchical PCL–PANI core–shell fiber obtained at the polymerization time of **a** 1 h, **b** 2 h, **c** 4 h and **d** 6 h, respectively.

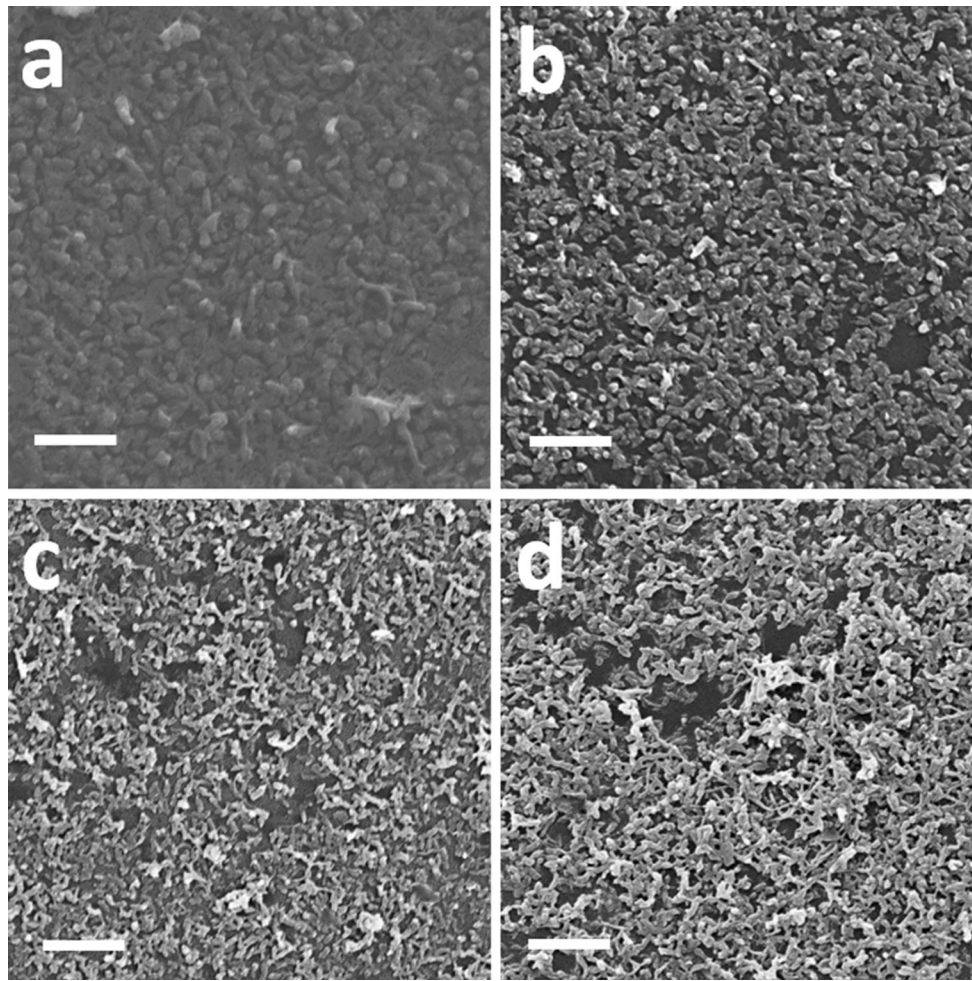


**Figure 6** SEM images of pure PANI film polymerized on the glass substrate with the deposition time of **a** 1 h, **b** 2 h, **c** 4 h and **d** 6 h, respectively. The scale bar is 1  $\mu\text{m}$ .

fibers can be obtained. Figure 7a, c shows the typical SEM images of the resulting smooth fibers with the diameter of 400 nm and 4  $\mu\text{m}$ , respectively. Different fiber width is realized by adjusting the electrospinning voltage (17 kV in the case of 400 nm vs 11 kV in the case of 4  $\mu\text{m}$ ). PANI is then deposited onto the surface of the smooth fibers by oxidative polymerization. As compared to the original fiber, the surface morphology of that after PANI deposition becomes rough, as can be seen from the SEM images shown in Fig. 7b, d.

In order to demonstrate the composition of the hierarchical PCL–PANI core–shell fiber, we have performed the FTIR and Raman measurement. Pure PCL fiber and pure PANI film are also measured for comparison. As shown in Fig. 8a black curve, PCL shows the characteristic peak at 1720  $\text{cm}^{-1}$ , which can be assigned to the stretching vibration of C=O

[20]. On the other hand, PANI exhibits the characteristic peaks at 3450 and 1300  $\text{cm}^{-1}$ , corresponding to the N–H stretching and C–N secondary amine stretching, respectively. Peaks at 1585 and 1494  $\text{cm}^{-1}$  originate from the C=C stretch of quinoid and benzenoid ring (Fig. 8a blue curve) [21]. For the PCL–PANI hierarchical fiber, it contains all the characteristic peaks from both PCL and PANI, as shown in Fig. 8a red curve. In the Raman spectra, PCL shows the characteristic peaks at 1730  $\text{cm}^{-1}$  (C=O) and 950  $\text{cm}^{-1}$  (C–COO) (Fig. 8b black curve) [22]. The characteristic peaks from PANI can be observed (Fig. 8b blue curve) at 418  $\text{cm}^{-1}$  (out-of-plane C–H wag), 520  $\text{cm}^{-1}$  (out-of-plane C–N–C torsion), 816  $\text{cm}^{-1}$  (imine deformation), 1186  $\text{cm}^{-1}$  (in-plane C–H bending), 1334  $\text{cm}^{-1}$  (C–N<sup>+</sup> stretching), 1501  $\text{cm}^{-1}$  (C=N stretching of quinoid) and 1593  $\text{cm}^{-1}$  (C–C stretching of benzoid), respectively

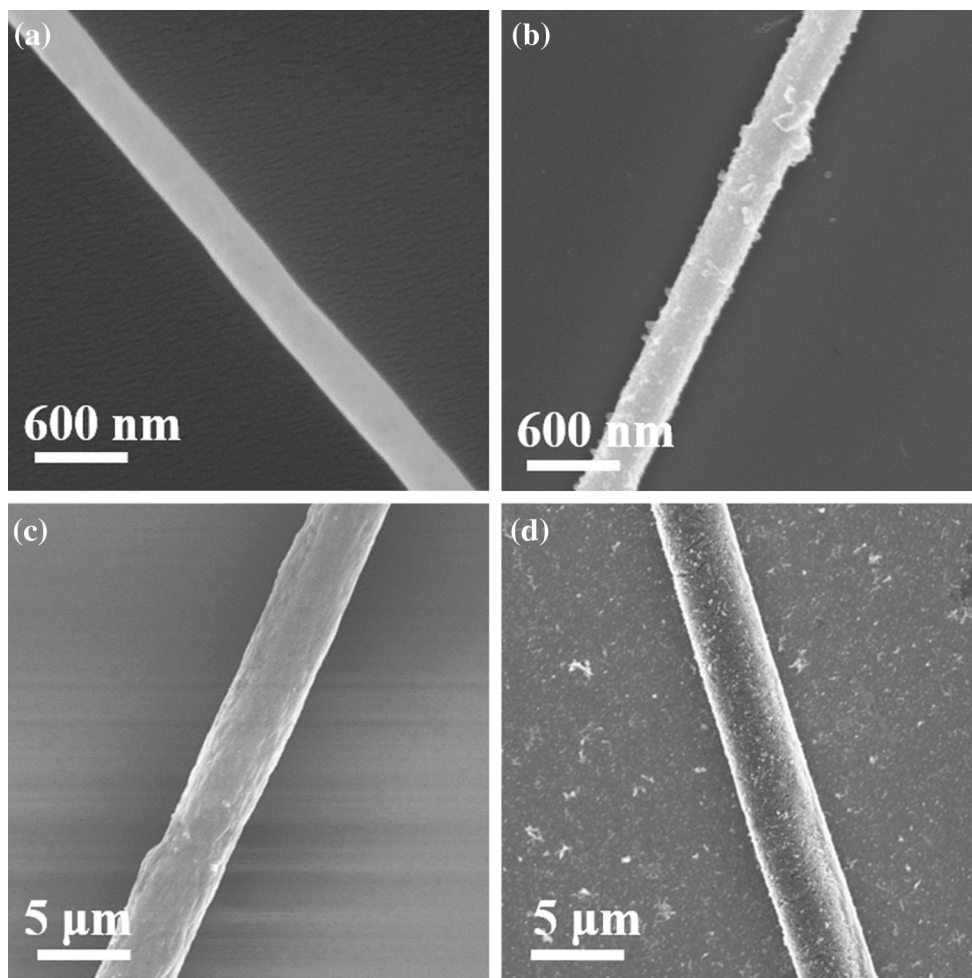


**Figure 7** SEM images of one 400-nm-diameter smooth fiber **a** before and **b** after PANI deposition. SEM images showing a 4- $\mu\text{m}$ -diameter smooth fiber **c** before and **d** after PANI deposition. The deposition time is 4 h.

**Figure 8 a** FTIR and **b** Raman spectra of the hierarchical PCL–PANI core–shell fibers (*red curve*), PANI film (*blue curve*) and PCL fibers (*black curve*).

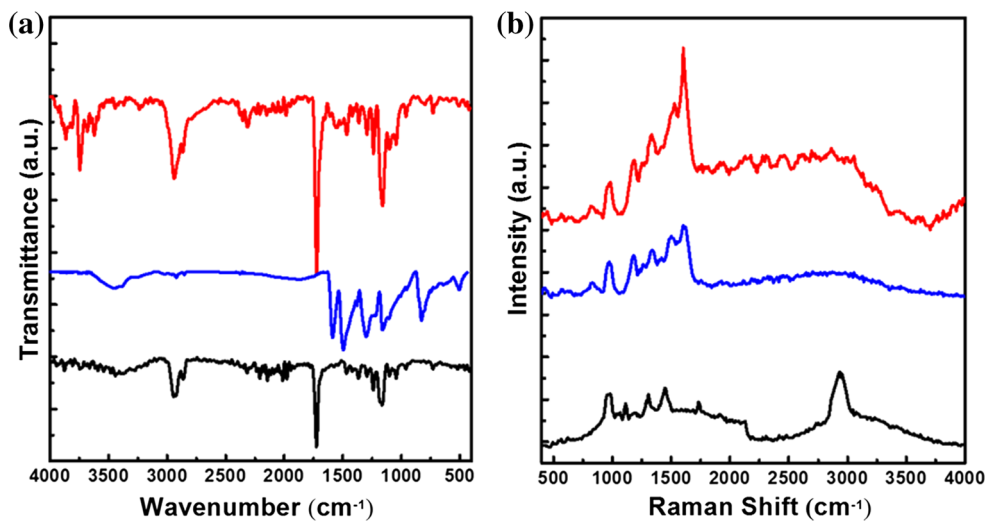
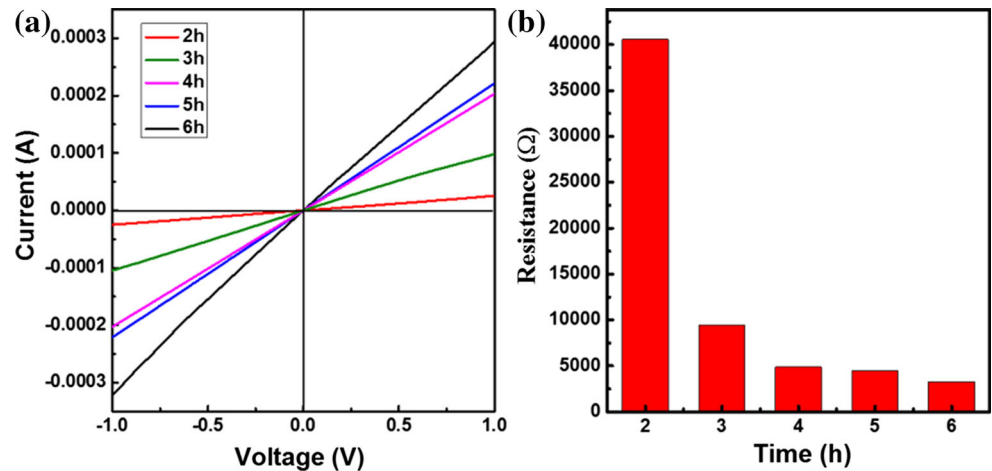




**Figure 9** **a** I–V characteristics and **b** the corresponding resistance of the PCL–PANI fiber mat with different PANI deposition time.



[23]. As can be seen in Fig. 8b red curve, the hierarchical PCL–PANI fiber contains all the characteristic peaks from PCL and PANI. These spectrum measurements thus confirm the chemical composition of the hierarchical core–shell fiber.

Furthermore, we have measured the conductivity of various fiber structures by placing them in between two electrodes. Pure PCL is non-conductive, while after the deposition of PANI, the conductivity of the fiber increases dramatically. Figure 9a shows the I–V characteristics of the PCL–PANI fibrous structures with different PANI polymerization time. The corresponding resistance is shown in Fig. 9b. The PCL–PANI fiber obtained at 2-h deposition time has a resistance of around 40 kΩ. As the polymerization time increases, the conductivity of the PCL–PANI fiber rises accordingly. The lowest resistance is observed for the fiber obtained at 6-h polymerization time, which is approximately 3.3 kΩ.

Furthermore, we have evaluated the sensing performance of the PCL–PANI hierarchical fiber by exposing it to the ammonia gas. The adsorption of ammonia on the PANI surface leads to the deprotonation process (Fig. 10a, b), which increases its resistance. Based on this principle, we are capable of evaluating the sensitivity of the sensing device by calculating the resistance changes before and after the ammonia exposure according to the following equation:  $S = (R_g - R_0)/R_0 = \Delta R/R_0$ , where  $S$  is the sensitivity;  $R_0$  and  $R_g$  are the resistance before and after ammonia gas exposure, respectively. Figure 10c red column shows the sensing behavior of hierarchical PCL–PANI fiber obtained at different polymerization times (the ammonia gas concentration is 50 ppm). The highest gas sensitivity of 8.4 is obtained for the

hierarchical fiber obtained at 4-h polymerization time. The high sensitivity comes from the high surface area-to-volume ratio caused by the hierarchical fibers, which contains both the porous structures and the spinous protrusions (Fig. 3c). Furthermore, we have compared the sensitivity of the hierarchical PCL–PANI fibers with those of the pure PANI film and the smooth PCL–PANI fiber counterparts with different diameter (Fig. 7). As can be seen from Fig. 10c purple, blue and green columns, due to the low surface area-to-volume ratio, both the film and the smooth fiber counterparts exhibit much lower sensitivity. The above results thus demonstrate the superiority of the hierarchical structure. In addition, we have evaluated the real-time sensing performance of the hierarchical PCL–PANI fiber. The ammonia gas is on for 4 min and off for 5 min. As can be seen from Fig. 10d, the resistance of hierarchical PCL–PANI fiber increases sharply within 20 s upon the exposure to the ammonia gas, indicating the fast response of the current sensor. Upon the removal of the ammonia gas, its resistance quickly drops to the original level, which shows the sensor is fully recovered. In addition, as can be seen from Fig. 10d inset, the PCL–PANI core–shell fiber shows negligible sensitivity toward 0.5 ppm ammonia gas. The detection limit of this sensor is estimated to be around 1 ppm. At 1 ppm, the sensor is still capable of exhibiting sensitivity as high as 0.94.

We have evaluated the repeatability of the current sensor. To this end, we have repetitively exposed it to the ammonia gas with a concentration of 10 ppm. The ammonia gas is applied for 20 s and turned off for another 20 s for the sensor to recover. The ammonia gas is switched on–off–on for several

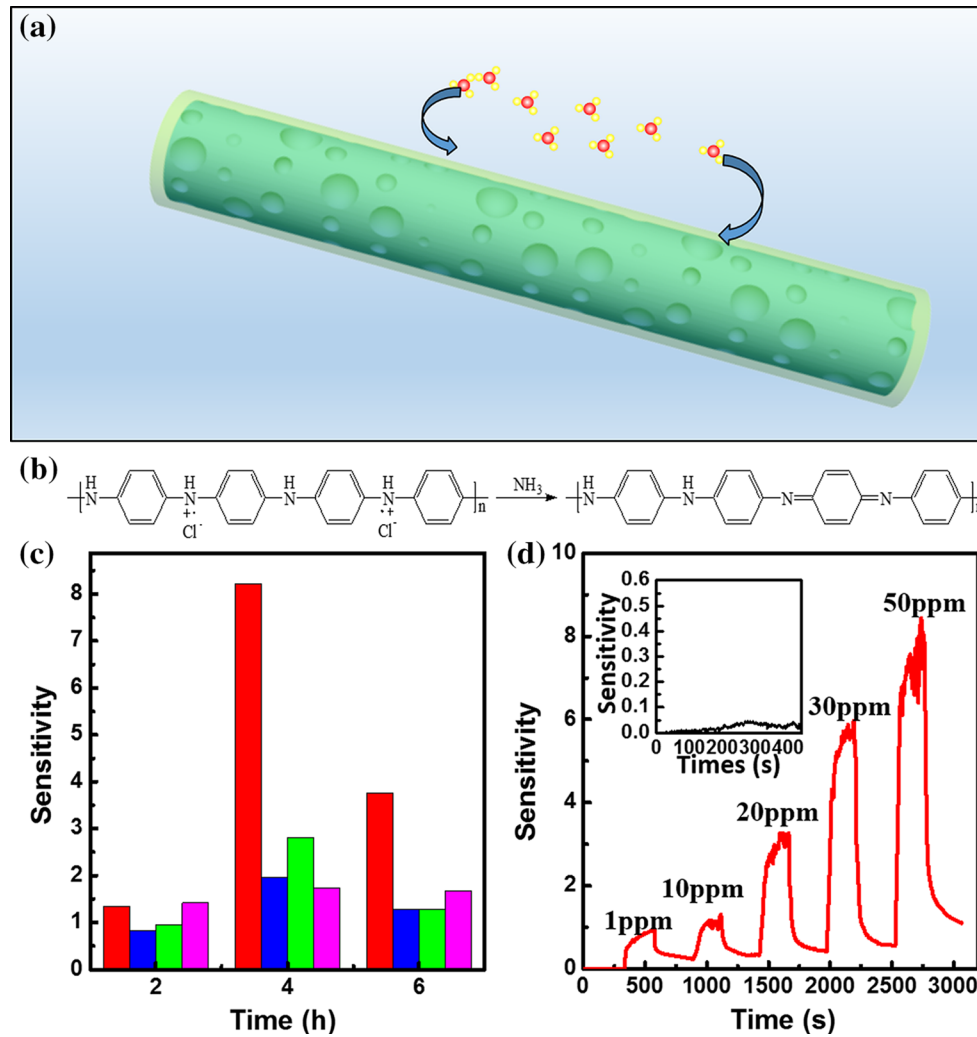


**Figure 10** a Schematic showing the sensing mechanism. b Chemical structure changes of PANI after ammonia gas exposure. c Sensitivity of PCL-PANI fiber obtained with different PANI deposition time. The ammonia concentration is fixed at 50 ppm. The sensitivity is compared for pure PANI (purple column) and PANI deposited on porous fiber (red column), 400-nm (green

column) and 4-μm (blue column) diameter smooth fiber, respectively. d The sensitivity of the hierarchical PCL-PANI core-shell fiber obtained at a polymerization time of 4 h when exposed to different concentrations of ammonia gas. Inset sensitivity of the hierarchical PCL-PANI core-shell fiber obtained at a polymerization time of 4 h when exposed to 0.5 ppm ammonia gas.

cycles. As can be seen from Fig. 11a, the resistance rises dramatically after the ammonia exposure; it can be recovered to the original value upon the ammonia removal. This process can be repeated for multiple cycles, indicating the good repeatability. Furthermore, we have studied the selectivity of the current sensor. We have tested its sensing performance toward a variety of gas analytes ranging from methanol, ethanol, acetone, isopropanol to dichloromethane and acetic acid. The concentrations of all gases are fixed at 50 ppm. It can be seen from Fig. 11b that the current sensor shows negligible response

toward these chemicals. This indicates the sensor reported in the current study can be utilized to selectively detect ammonia gas.

Furthermore, we have studied the repeatability of the fiber-based sensor after long-term storage. Figure 12a, b shows the sensing performance of PCL-PANI core-shell fiber after being placed in air for 7 days and 3 months, respectively. The sensor has good stability after long-term use with fast response and good reversibility. The sensitivity only shows a little decrease, indicating the sensor has good repeatability after long-term storage. This result is

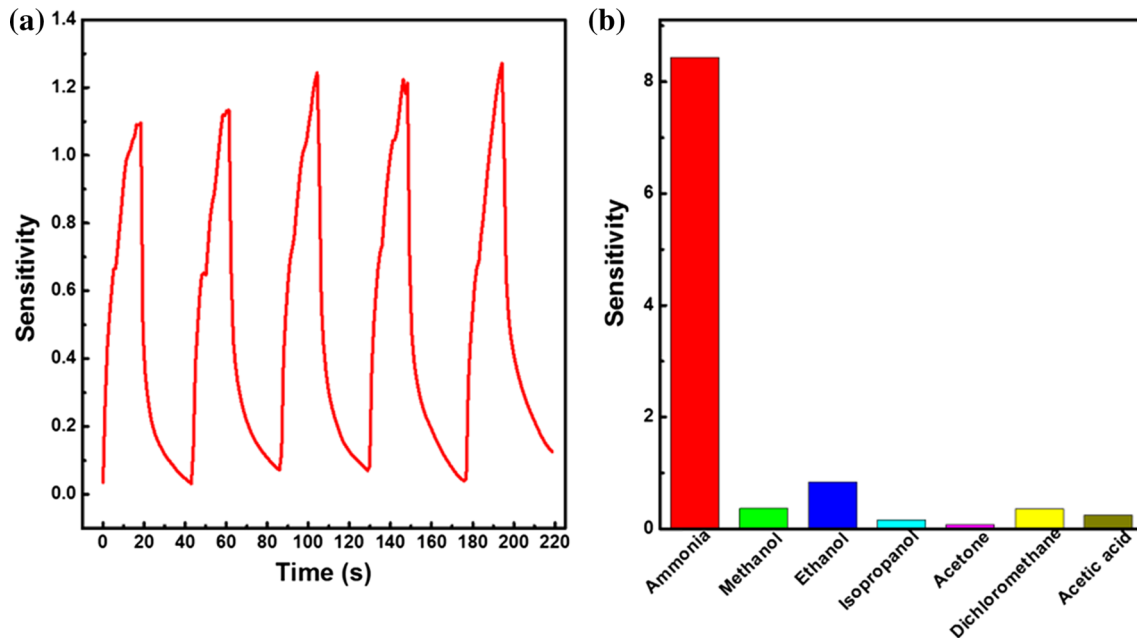
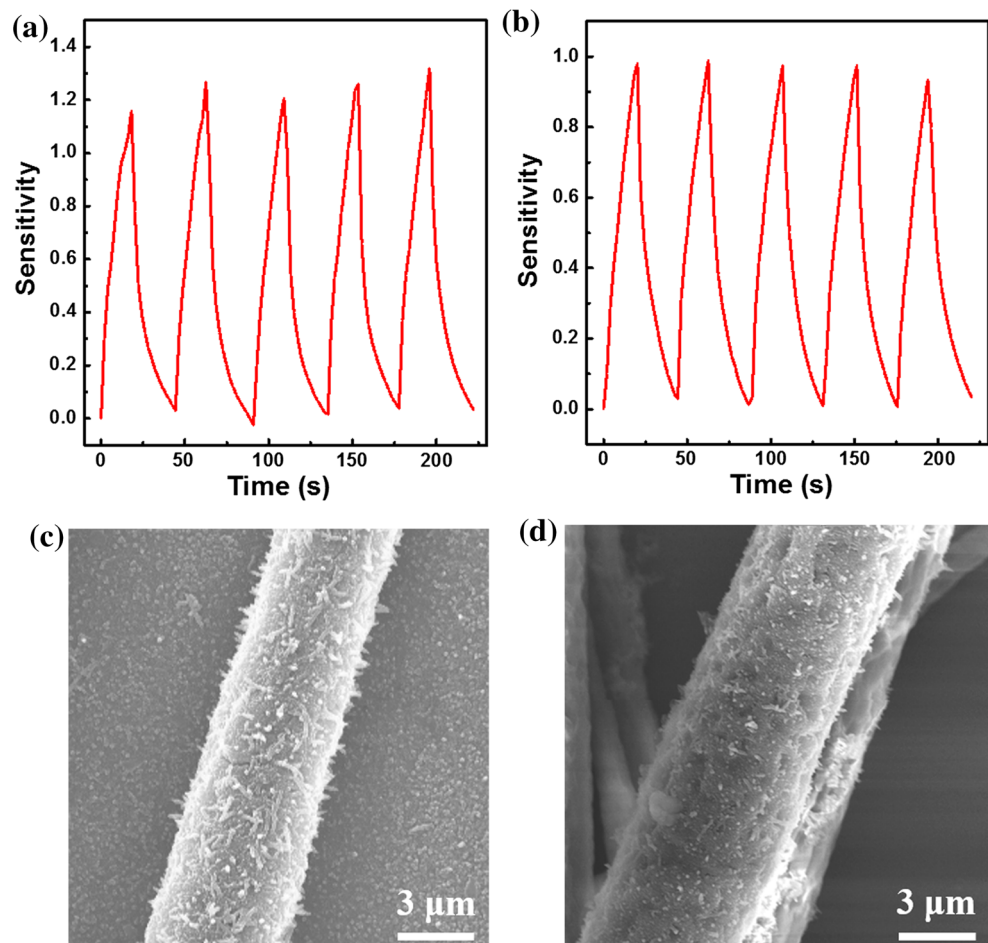


**Figure 11** **a** Repeatability of the PCL-PANI fiber-based sensor. The ammonia gas (10 ppm) is on for 20 s and off for 20 s. **b** Gas-sensing selectivity of the current sensor toward ammonia over other volatile organic gases. The concentrations of all gases are 50 ppm.

**Figure 12** Repeatability of the PCL-PANI core-shell fiber-based sensor after **a** 7 days and **b** 3 months, respectively. The ammonia gas concentration is 10 ppm. SEM images show the hierarchical structures of PCL-PANI core-shell fibers after **c** 7 days and **d** 3 months.



consistent with that reported in the literature [24]. Furthermore, we have characterized the structure of PCL–PANI core–shell fiber after 7 days and 3 months. It can be seen from the SEM images shown in Fig. 12c, d that the spinous structures remain unchanged after long-term storage, indicating the good stability of PCL–PANI core–shell fiber in air.

## Conclusions

In conclusion, by combining oxidative polymerization with electrospinning, we have generated a PCL–PANI core–shell fiber with hierarchical structures. The hierarchical structure is obtained by in situ polymerization of aniline on the surface of porous PCL electrospun fibers. Due to the high specific area originating from the hierarchical structure, when utilized as the ammonia gas sensor, the resulting structure exhibits a high sensitivity, which is far superior to that of the smooth fibers or the film counterpart. In addition, the ammonia gas sensor based on the current hierarchical structure shows a low detection limit, fast responsibility, good repeatability and selectivity. We thus believe hierarchical PCL–PANI fiber may have potential application in the ammonia-gas-sensing field.

## Acknowledgements

This work was supported by the National Natural Science Foundation of China (Grant Nos. 21574094, 21304064), the Natural Science Foundation of Jiangsu Province (Grant Nos. BK20130292, BK20150314), Collaborative Innovation Center (CIC) of Suzhou Nano Science and Technology and a Project Funded by the Priority Academic Program Development of Jiangsu Higher Education Institutions (PAPD), the Fund for Excellent Creative Research Teams of Jiangsu Higher Education Institutions and the project-sponsored by SRF for ROCS, SEM.

## References

- [1] Yang XN, Loos J, Veenstra SC, Verhees WJH, Wienk MM, Kroon JM, Michels MAJ, Janssen RAJ (2005) Nanoscale morphology of high-performance polymer solar cells. *Nano Lett* 5:579–583
- [2] Chen J, Liu Y, Minett AI, Lynam C, Wang JZ, Wallace GG (2007) Flexible, aligned carbon nanotube/conducting polymer electrodes for a lithium-ion battery. *Chem Mater* 19:3595–3597
- [3] Bai H, Shi GQ (2007) Gas sensors based on conducting polymers. *Sensors* 7:267–307
- [4] Timmer B, Olthuis W, van den Berg A (2005) Ammonia sensors and their applications—a review. *Sens Actuators B Chem* 107:666–677
- [5] Chang QF, Zhao K, Chen X, Li MQ, Liu JH (2008) Preparation of gold/polyaniline/multiwall carbon nanotube nanocomposites and application in ammonia gas detection. *J Mater Sci* 43:5861–5866. doi:10.1007/s10853-008-2827-3
- [6] Nicolas-Debarnot D, Poncin-Epaillard F (2003) Polyaniline as a new sensitive layer for gas sensors. *Anal Chim Acta* 475:1–15
- [7] Huang JX, Kaner RB (2006) The intrinsic nanofibrillar morphology of polyaniline. *Chem Commun* 367–376
- [8] Huang JX, Virji S, Weiller BH, Kaner RB (2003) Polyaniline nanofibers: facile synthesis and chemical sensors. *J Am Chem Soc* 125:314–315
- [9] Wan PB, Wen XM, Sun CZ, Chandran BK, Zhang H, Sun XM, Chen XD (2015) Flexible transparent films based on nanocomposite networks of polyaniline and carbon nanotubes for high-performance gas sensing. *Small* 11:5409–5415
- [10] Yin ZG, Zheng QD (2012) Controlled synthesis and energy applications of one-dimensional conducting polymer nanostructures: an overview. *Adv Energy Mater* 2:179–218
- [11] Dong B, Gwee L, Salas-de la Cruz D, Winey KI, Elabd YA (2010) Super proton conductive high-purity nafion nanofibers. *Nano Lett* 10:3785–3790
- [12] Dong B, Smith ME, Wnek GE (2009) Encapsulation of multiple biological compounds within a single electrospun fiber. *Small* 5:1508–1512
- [13] Shadi L, Karimi M, Ramazani S, Entezami AA (2014) Preparation of electrospun nanofibers of star-shaped polycaprolactone and its blends with polyaniline. *J Mater Sci* 49:4844–4854. doi:10.1007/s10853-014-8185-4
- [14] Khattab TA, Abdelmoez S, Klapotke TM (2016) Electrospun nanofibers from a tricyanofuran-based molecular switch for colorimetric recognition of ammonia gas. *Chem Eur J* 22:4157–4163
- [15] Liu HQ, Kameoka J, Czaplewski DA, Craighead HG (2004) Polymeric nanowire chemical sensor. *Nano Lett* 4:671–675
- [16] Shenoy SL, Bates WD, Frisch HL, Wnek GE (2005) Role of chain entanglements on fiber formation during electrospinning of polymer solutions: good solvent, non-specific polymer-polymer interaction limit. *Polymer* 46:3372–3384

- [17] Liu LM, Liu M, Su YJ, Dong YG, Zhou W, Zhang LN, Zhang H, Dong B, Chi LF (2015) Tadpole-like artificial micromotor. *Nanoscale* 7:2276–2280
- [18] Liu LM, Dong YG, Sun YY, Liu M, Su YJ, Zhang H, Dong B (2016) Motion-based pH sensing using spindle-like micromotors. *Nano Res* 9:1310–1318
- [19] Bognitzki M, Czado W, Frese T, Schaper A, Hellwig M, Steinhart M, Greiner A, Wendorff JH (2001) Nanostructured fibers via electrospinning. *Adv Mater* 13:70–72
- [20] Lee EJ, Teng SH, Jang TS, Wang P, Yook SW, Kim HE, Koh YH (2010) Nanostructured poly( $\epsilon$ -caprolactone)–silica xerogel fibrous membrane for guided bone regeneration. *Acta Biomater* 6:3557–3565
- [21] Konwer S, Guha AK, Dolui SK (2013) Graphene oxide-filled conducting polyaniline composites as methanol-sensing materials. *J Mater Sci* 48:1729–1739. doi:[10.1007/s10853-012-6931-z](https://doi.org/10.1007/s10853-012-6931-z)
- [22] Taddei P, Tinti A, Reggiani M, Fagnano C (2005) In vitro mineralization of bioresorbable poly( $\epsilon$ -caprolactone)/apatite composites for bone tissue engineering: a vibrational and thermal investigation. *J Mol Struct* 744–747:135–143
- [23] Guo YL, Wang T, Chen FH, Sun XM, Li XF, Yu ZZ, Wan PB, Chen XD (2016) Hierarchical graphene-polyaniline nanocomposite films for high-performance flexible electronic gas sensors. *Nanoscale* 8:12073–12080
- [24] Zhao J, Wu G, Hu Y, Liu Y, Tao X, Chen W (2015) A wearable and highly sensitive CO sensor with a macroscopic polyaniline nanofiber membrane. *J Mater Chem A* 3:24333–24337